

Source apportionment of PM_{2.5} in Seoul, Korea

J.-B. Heo¹, P. K. Hopke², and S.-M. Yi¹

¹Department of Environmental Health, School of Public Health, Seoul National University, Seoul, Korea

²Department of Chemical and Biomolecular Engineering, Clarkson University, Potsdam, NY, USA

Received: 27 August 2008 – Published in Atmos. Chem. Phys. Discuss.: 8 December 2008

Revised: 9 June 2009 – Accepted: 10 July 2009 – Published: 27 July 2009

Abstract. PM_{2.5} samples were collected at a centrally located urban monitoring site in Seoul, Korea, every third day from March 2003 to December 2006 and analyzed for their chemical constituents. Sources were identified using positive matrix factorization (PMF). A total of 393 samples were obtained during the sampling period, and 20 chemical species were measured. Nine PM_{2.5} source categories were identified providing physically realistic profiles and interesting insights into the source contributions to the ambient mass concentrations. The major contributors of PM_{2.5} were secondary nitrate (20.9%), secondary sulfate (20.5%), gasoline-fueled vehicles (17.2%), and biomass burning (12.1%), with lesser contributions from diesel emissions (8.1%), soil (7.4%), industry (6.7%), road salt and two-stroke vehicles (5.1%), and aged sea salt (2.2%). PM_{2.5} levels in Seoul were influenced by both local urban activities and regional-scale transport. Conditional probability function (CPF) results identified possible source directions of local sources such as motor vehicles (gasoline and diesel), industry, and road salt. Potential source contribution function (PSCF) results showed that possible source areas contributing to the elevated secondary particle concentrations (sulfate and nitrate) in Seoul to be the major industrial areas in China.

therefore more likely to increase the incidence of respiratory and cardiovascular disease (Dockery et al., 1993; Schwartz et al., 2002). For this reason, the United States Environmental Protection Agency (EPA) promulgated a national ambient air quality standard for particles with a diameter of $\leq 2.5 \mu\text{m}$ (PM_{2.5}) since 1997, and in 2006 the EPA reduced the 24-h PM_{2.5} standard to a level of $35 \mu\text{g m}^{-3}$ (US Federal Register, 2007).

Recently, environmental health problems arising from exposure to fine particulate matter (PM_{2.5}) have been identified in many parts of Korea (Kim et al., 2007). However, PM_{2.5} is not properly managed in Korea because of a lack of systematic approaches to study it. The capital city of Seoul has severe air pollution problems, and a variety of governmental policies, such as expansion of the use of liquefied natural gas and low-sulfur fuels and movement of industrial sources out of the city, have been implemented to improve urban air quality. As a result, concentrations of ambient air pollutants (particularly SO₂) have been significantly reduced since 1996–1997. On 1 January 2005, the Korean Ministry of Environment established the “Special Act on Metropolitan Air Quality Improvement” whose principal objective is to improve the PM₁₀ annual concentration in Seoul metropolitan area from $60 \mu\text{g/m}^3$ in 2005 to $40 \mu\text{g/m}^3$ by 2014. However, the PM_{2.5} concentrations remains high compared to similar cities in developed countries (Kang et al., 2006; Kim et al., 2007).

Source apportionment methods provide tools to develop efficient and effective PM control strategies and to develop policy to prevent the general public’s exposure. Positive matrix factorization (PMF) is a development in the class of data analysis techniques called factor analysis (Paatero and Tapper, 1993, 1994), where the fundamental problem is to resolve the identities and contributions of components in an unknown mixture (Malinowski, 2002). PMF has been used as a source apportionment tool in many air quality studies (Kim and Hopke, 2004a, b; Kim et al., 2004a, b, 2007; Lee and Hopke, 2006; Hwang and Hopke, 2007; Lanz et al., 2007;

1 Introduction

Airborne particles play an important role in human health effects, visibility degradation, and global climate change. Previous epidemiological studies indicated statistical associations between mortality and morbidity and ambient concentrations of particulate matter (PM), particularly fine particles that can more readily penetrate into the lungs and are



Correspondence to: S.-M. Yi
(yiseung@snu.ac.kr)

Sunder Raman and Hopke, 2007; Ulbrich et al., 2009; Vianna et al., 2008). PMF results have been coupled with surface wind direction data to provide identification of the locations of local emission sources affecting a receptor site (Lee et al., 2006; Pekney et al., 2007). The addition of back-trajectory ensemble methods can help to identify regional sources that contribute to urban PM_{2.5} concentrations (Lee and Hopke, 2006; Kim et al., 2007). In East Asia, these trajectory ensemble methods have been successfully used to identify possible source locations for the dry deposition of heavy metals (Han et al., 2004) and PM_{2.5} chemical species (Kang et al., 2006; Kim et al., 2007). However, in these earlier studies, trajectory analysis was not combined with source apportionments.

Several previous studies have identified possible sources of PM_{2.5} in Seoul using the chemical mass balance (CMB) model (Park and Kim, 2005; Lee et al., 2005). However, some of the source profiles used in their CMB models were derived from sources in the United States and may not be directly applicable to Seoul. Unfortunately, source profile measurements are methodologically difficult and time-consuming to make. Factor analysis is a different but highly effective tool that can be used to apportion sources without directly interacting with the chemical profiles. It offers an alternative in Korea where there is no local source profile library.

The objectives of this study were to investigate the source profiles and the source contributions of PM_{2.5} in Seoul using PMF and to determine the impact of the regional transport of PM_{2.5} sources on the air quality in Seoul. The results of this study can be used to establish an effective management strategy of the air quality and adverse health effects stemming from PM_{2.5} in Korea.

2 Experimental methods

2.1 Sampling and analysis

Ambient air samples were collected every third day over a 24-h period from March 2003 to December 2006. The measurement site was located on the roof (~17 m above ground, 37.5° N, 127.00° E) of the School of Public Health building at Seoul National University, a mixed commercial and residential area in Seoul, Korea (Fig. 1). Filter samples were simultaneously collected using a 4-channel system. The system had two channels using an Annular Denuder System (ADS) and two channels using filter packs (URG) that collected samples for the analysis of PM_{2.5} gravimetric concentration, water-soluble ionic species, carbonaceous species (organic carbon and elemental carbon), and trace elements.

The 4-channel system consisted of size-selective inlets, four cyclones (URG-2000-30EH and 30EN, URG) to provide a particle size cutoff based on the flow rate, the collection substrates, critical orifices that provided the proper flow rate for the desired particle size cutoff, and four vac-

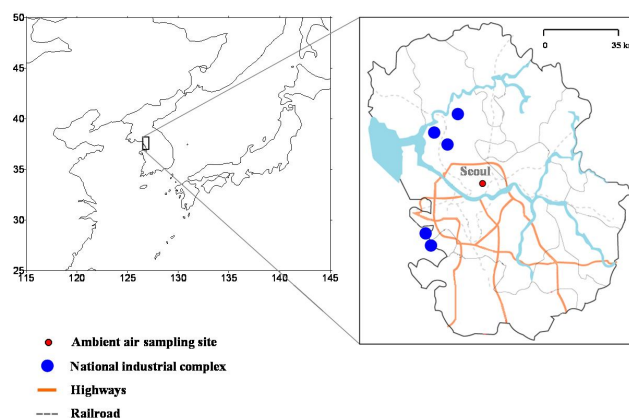


Fig. 1. Map of Seoul metropolitan area including the sampling site and selected industrial areas relevant to the source apportionments presented in this study.

uum pumps. The flow rate was monitored for each channel by independent dry gas meters. Ionic constituents were measured in the two channels using the ADS that operated using a 10.0 L/min flow rate. The ADS consisted of two annular denuders coated with sodium carbonate and citric acid to collect acidic (SO₂, HNO₃) and basic (NH₃) gases followed by a Zefluor filter (47 mm Pall Life Sciences, 2 μm pore size) located downstream of the denuder. These samples were used to determine water-soluble ionic species. The Zefluor filters were followed by Nylasorb membrane filters (47 mm Gelman Science, 1 μm pore size) for the accurate measurement of volatilized nitrate and paper filters (47 mm Whatman International Ltd.) coated with citric acid, to correct for the volatilized ammonium. After sampling, reagent-grade deionized water was used to extract the annular denuders, and ion chromatography eluent solution was used to extract the filters. Extracted solutions were analyzed with Dionex DX-120 Ion Chromatograph.

Teflon filters (25 mm Gelman Teflo, 3 μm pore size) were collected at 16.7 L/min flow rate for PM_{2.5} gravimetric mass and for the measurement of trace elements. The PM_{2.5} mass was obtained by weighing the Teflon filters using a microbalance (Sartorius, 10 mg reading precision). These filters were then used to determine trace elements using proton induced x-ray emission (PIXE). Another filter holder with a flow rate of 16.7 L/min was used to collect quartz filter samples for organic carbon and elemental carbon analysis. These 47-mm quartz filters were pre-baked at 550°C for 12 h to lower their carbon blanks, and analyzed using the NIOSH TOT (Thermal/Optical Transmittance) method (Birch and Cary, 1996).

For quality assurance in the analysis of the samples, another 16 blank filters were simultaneously examined using the same methods as described above. Background contamination was periodically monitored using field blanks that were simultaneously processed with the field samples and

filter blanks. For all analytes, background contamination was less than 5% of associated samples. Recovery efficiencies were determined by spiking one out of every 10 samples and reproducibility tests were performed by replicate analysis one out of every 10 samples. Recovery efficiencies varied between 95% and 105%, and reproducibility tests had acceptable results within $\pm 10\%$ for all the chemical species. Detection limits were calculated as concentrations corresponding to two times the uncertainty of each chemical species measured on the field blanks.

Meteorological data including temperature, relative humidity, wind speed, and wind direction were recorded every 5 min using a meteorological tower (Davis Instrument) at the sampling site.

2.2 Receptor modeling

Receptor modeling is based on the idea that mass conservation can be assumed and a mass balance analysis can be used to identify and apportion sources of airborne PM in the atmosphere (Hopke, 1991). Positive Matrix Factorization (PMF) model (Paatero and Tapper, 1994; Paatero, 1997) is an advanced receptor model based on least-squares techniques that uses error estimates of the measured data to provide weights in the fitting process. The notation of the PMF is

$$x_{ij} = \sum_{k=1}^p g_{ik} \cdot f_{kj} + e_{ij}, \quad (1)$$

where x_{ij} is the j -th species concentration measured in the i -th sample, g_{ik} is the particulate mass concentration from the k -th source contributing to the i -th sample, f_{kj} is the mass fraction of the j -th species from the k -th source, and e_{ij} is residuals associated with the j -th species concentration measured in the i -th sample, and p is the total number of independent sources. Non-negativity constraints are used on the PMF factors, g_{ik} and f_{kj} , to decrease rotational freedom. PMF provides a solution that minimizes an object function, $Q(E)$, based upon the uncertainties of each observation (Polissar et al., 1998). This function is defined as

$$Q(E) = \sum_{i=1}^n \sum_{j=1}^m \left[\frac{x_{ij} - \sum_{k=1}^p g_{ik} f_{kj}}{u_{ij}} \right]^2, \quad (2)$$

where u_{ij} is an uncertainty estimate for the j -th constituent measured in the i -th sample.

The application of PMF depends on estimated uncertainties for each observation. The uncertainty estimation method provides a useful tool for decreasing the weight of missing and below-detection-limit data in the solution. The procedure of Polissar et al. (1998) was applied to allocate observed data and associated uncertainties as input into the PMF analysis. The concentration values were used for the measured data, and the sum of the analytical uncertainty and 1/3 of

the methods detection limits (MDL) value were used as the overall uncertainty assigned to each observation. Values below the MDL were replaced by half of the MDL, and their overall uncertainties were set at 5/6 of the MDL. Missing values were replaced by the geometric mean of the measured values, and associated uncertainties were set at four times the geometric mean. In addition to the standard uncertainty estimation, the uncertainty must take into account the measurement uncertainty as well as the temporal variability in the source profiles over the monitoring period.

In several cases, in order to take the temporal variability into account, larger uncertainties were used to decrease the weight of some specific variables in model fitting (Paatero and Hopke, 2003). Uncertainties were increased by a factor of three for OC, EC, and NO_3^- for which the signal-to-noise (SN) ratio were between 0.2 and 2. The estimated uncertainties of Ni and Br that had below MDL values nearly 40% were increased by factor of two to reduce their weight in the solution. To achieve the optimal solution, the PMF was run using different initial seeds for the iterative fitting process, and solutions with different numbers of sources were examined. The robust mode was used to reduce the effects of extreme values on the PMF solution. The estimated uncertainties of extreme values were increased to downweight those concentrations. To reduce the rotational ambiguity, a matrix of FPEAK and FKEY values were used in this study (Paatero et al., 2002).

Kim and Hopke (2004a, b) used an alternative approach to the conventional multiple linear regression of model-resolved factor contributions against observed mass for normalization of the factor profiles and contributions in order to treat the mass closure issue. They included the measured PM_{2.5} mass concentration as an input variable in the PMF analysis, with the estimated uncertainties of PM_{2.5} concentrations of four times the measured value. PMF then apportioned the PM_{2.5} contribution for each source according to its temporal variation. This procedure was used for normalization in this analysis.

2.3 Hybrid receptor models

2.3.1 Conditional probability function (CPF)

To estimate the local source impacts from various wind directions, the CPF (Kim et al., 2003) was performed for each source using the source contributions estimated from the PMF coupled with the surface wind direction data. The daily fractional mass contributions of each source relative to the total of the sources were used rather than the absolute contributions to minimize the effect of atmospheric dilution. The same daily fractional contribution was assigned to each hour of a given day to match the hourly wind data. The CPF was defined as:

$$\text{CPF}_{\Delta\theta} = \frac{m_{\Delta\theta}}{n_{\Delta\theta}}, \quad (3)$$

where $m_{\Delta\theta}$ is the number of occurrence from wind sector $\Delta\theta$ that exceeded the threshold criterion, and $n_{\Delta\theta}$ is the total number of data from the same wind sector. In this study, 16 sectors ($\Delta\theta=22.5^\circ$) were chosen and calm winds ($\leq 1 \text{ ms}^{-1}$) were excluded from this analysis because of the isotropic behavior of the wind vane caused by calm winds. The threshold criterion was set at the upper 20th percentile value of the fractional source contributions for each source.

2.3.2 Potential source contribution function (PSCF)

To estimate the likely source locations for long-range transporting aerosols, the PSCF (Ashbaugh et al., 1985; Hopke et al., 1995) was calculated using the daily source contributions deduced from the PMF and backward trajectories, calculated using the Hybrid Single Particle Lagrangian Integrated Trajectory (HYSPPLIT) model and gridded FNL global meteorological data (Draxler and Rolph, 2007). If a trajectory end point of the air parcel lies in a geophysical grid cell, the trajectory was assumed to collect PM_{2.5} emitted in that cell. Once the PM_{2.5} was incorporated into the air parcel, it was assumed to be transported along the trajectory to the monitoring site. PSCF_{*ij*} is the conditional probability that an air parcel that passed through the *ij*-th cell had a high concentration upon arrival to the monitoring site and was defined as

$$\text{PSCF}_{ij} = \frac{m_{ij}}{n_{ij}}, \quad (4)$$

where n_{ij} is the total number of end points that fall in the *ij*-th cell, and m_{ij} is the number of end points in the same cell that are associated with samples that exceeded the threshold criteria.

Typically for long range transport (>24 h), trajectories that have started at different heights may vary significantly because backward trajectories started at different heights traverse different distances and pathways (Hsu et al., 2003). In this study, multiple-heights PSCF was performed to reduce this uncertainty. The average contribution of each source was used for the threshold criterion. Five-day backward trajectories starting at every hour at a height of 100, 500, 1000, and 1500 m above ground level were computed using the vertical velocity model for every sample day, producing 120 hourly trajectory end points per sample. The geophysical region covered by the trajectories was divided into 8400 grid cells of $1^\circ \times 1^\circ$ latitude and longitude, for an average of 550 trajectory end points per cell. The sources were likely to be located in the area that had high PSCF values.

To minimize the effect of small n_{ij} values resulting in high PSCF values with high uncertainties, an arbitrary weight function $W(n_{ij})$ was applied to downweight the PSCF values for the cell in which the total number of end points was

less than three times the average number of end points per cell (Hopke et al., 1995; Polissar et al., 2001):

$$W(n_{ij}) = \begin{cases} 1.0, & 1600 < n_{ij} \\ 0.7, & 700 < n_{ij} \leq 1600 \\ 0.4, & 500 < n_{ij} \leq 700 \\ 0.2, & 500 \geq n_{ij} \end{cases}, \quad (5)$$

3 Results and discussion

3.1 PM_{2.5} mass concentrations and chemical compositions

A total of 393 samples analyzed for 20 chemical species were collected between March 2003 and December 2006 and used in the data analysis. Time series plot of measured PM_{2.5} speciation data in this study is shown in Supplemental Fig. S1 (see <http://www.atmos-chem-phys.net/9/4957/2009/acp-9-4957-2009-supplement.pdf>). The annual average PM_{2.5} concentration was $43.5 \mu\text{g m}^{-3}$ that is almost three times higher than the US NAAQS annual PM_{2.5} standard of $15 \mu\text{g m}^{-3}$. The mass fraction of OC, SO₄²⁻, NO₃⁻, NH₄⁺, EC, crustal trace elements, and non-crustal trace elements in PM_{2.5} accounted for 24.2%, 18.6%, 16.2%, 12.1%, 7.9%, 3.6%, and 3.0% of the total mass, respectively (Fig. S2). OC was the highest contributor to PM_{2.5} mass. During the study period, high mass concentration episodes (i.e. smog episodes which exceed the average daily PM_{2.5} mass of $65 \mu\text{g m}^{-3}$) and yellow sand events were observed on 64 days and 21 days, respectively. The PM_{2.5} mass concentrations and its constituents during smog episodes were about two to three times higher than those during non-smog episodes. Especially, the mass fractions of secondary aerosols such as sulfate, nitrate, and ammonium during the smog episodes were higher than those of the other constituents. Crustal trace elements concentrations were high during yellow sand events due to the long-range transport of dust particles from Eastern Mongolia and the Gobi Desert.

3.2 Determination of the number of factors

Table 1 contains the summary of statistics for the PM_{2.5} mass concentrations and the 20 chemical species. Because of the high correlation between the PIXE sulfur and the ion chromatography sulfate, the ion chromatography sulfate was used in the PMF analysis. Additionally, all variables with more than 80% of the values being below their respective detection limits were excluded from the analysis.

In order to select modeling parameters and the number of factors, the mathematical PMF diagnostics and interpretable testing of the plausibility of PMF solutions were explored. The PMF diagnostics (model error, Q , rotational ambiguity, rotmat, etc.) were based on Lee et al. (1999). Figure 2 shows the Q -value for the different number of factors and the FPEAK values and the variation of IM, IS, and rotational

Table 1. Summary statistics and mass concentrations of PM_{2.5} and the 20 species used in the PMF analysis.

| Species | Concentration (ng/m ³) | | | | Missing + BDLs ^b (%) | S/N Ratio ^c |
|-------------------------------|------------------------------------|--------------------|---------|---------|------------------------------------|---------------------------|
| | Geometric Mean ^a | Arithmetic Mean | Minimum | Maximum | | |
| PM _{2.5} | 37 616 | 43 502 | 5780 | 131 224 | 0 | – |
| OC | 9468 | 10 522 | 2126 | 27 927 | 0 | 1.5 |
| EC | 2914 | 3428 | 704 | 16 637 | 0 | 1.7 |
| SO ₄ ²⁻ | 5766 | 8109 | 13 | 47 976 | 0 | 3.4 |
| NO ₃ ⁻ | 5173 | 7057 | 58 | 41 376 | 0 | 1.2 |
| NH ₄ ⁺ | 3704 | 5268 | 13 | 25 469 | 0 | 4.3 |
| Na | 123 | 150 | 7.3 | 624 | 2.1 | 5.6 |
| Mg | 41 | 61 | 1.1 | 503 | 5.3 | 8.7 |
| Al | 185 | 262 | 18 | 2191 | 0 | 9.5 |
| Si | 505 | 707 | 52 | 5956 | 0 | 9.5 |
| Cl | 166 | 479 | 0.8 | 4838 | 3.4 | 9.9 |
| K | 331 | 409 | 46 | 2171 | 0 | 9.2 |
| Ca | 143 | 191 | 19 | 1493 | 0 | 9.4 |
| Ti | 17 | 25 | 0.3 | 192 | 5.3 | 9.1 |
| Mn | 14 | 19 | 0.2 | 125 | 0.8 | 4.9 |
| Fe | 300 | 364 | 52 | 2220 | 0 | 9.1 |
| Ni | 0.9 | 2.3 | 0.2 | 11 | 44 | 6.5 |
| Cu | 14 | 17 | 0.2 | 82 | 0.5 | 8.9 |
| Zn | 95 | 115 | 18 | 697 | 0 | 9.1 |
| Br | 3.8 | 10 | 0.5 | 58 | 38 | 6.6 |
| Pb | 32 | 51 | 0.9 | 302 | 9.5 | 8.6 |

^a Data below the limit of detection were replaced by half of the reported detection limit values for the geometric mean calculations.

^b Below detection limit.

^c Signal-to-Noise ratio.

freedom for the different number of factors chosen in PMF. As the number of factors approaches to a critical value, IM and IS will clearly decrease. Also, choosing the maximum element in rotmat will be the factor element with the highest rotational ambiguity. There was a significant increase in maximum rotmat element from nine factors to ten factors (Fig. 2). Moreover, biomass burning was not extracted in the eight factor model. In the ten factor model, two gasoline factor profiles were identified. Since the profile and contribution of two gasoline factors had similar patterns showing redundancy, the nine factor model was chosen based on its reasonable results. The nine factor model and the value of FPEAK = 0.0 provided the most physically meaningful solution and the best agreement between a calculated Q -value of 8090 and a theoretical Q of approximately 7860. For the FKEY matrix, a FKEY value of four was used to moderately pull ammonium down for the secondary nitrate and industry factor. The average source contributions of each factor to the total average PM_{2.5} mass concentration are presented in Table S1.

3.3 Source identification and apportionment

A comparison between the reconstructed and measured PM_{2.5} mass concentrations showed that the reconstructed sources effectively reproduced the measured values and accounted for most of the variation in the PM_{2.5} mass concentrations (slope = 0.89 ± 0.17, r^2 = 0.88; Fig. 3). The PMF-deduced source profiles (prediction values and error bars) and contributions are presented in Figs. 4 and 5, respectively.

The secondary nitrate factor is characterized by their high concentrations of NO₃⁻ and NH₄⁺ (Kim et al., 2003; Lee et al., 2006) and the molar ratio of ammonium to nitrate is 1.8. In this study, secondary nitrate factor accounted for 20.9% of the PM_{2.5} mass concentration at the monitoring site. As shown in Fig. 6, high mass concentrations from secondary nitrate factor were observed during the spring. In general, secondary nitrate formation depends on NO_x, NH₃, temperature, relative humidity, OH/radiation, and nighttime chemistry via NO₃ (g). Secondary nitrate varies seasonally, with higher concentrations in winter because of lower temperatures and higher humidity that facilitate the formation of secondary nitrate particles (Seinfeld and Pandis, 1998). Besides temporal variation by temperature, ammonia availability plays a

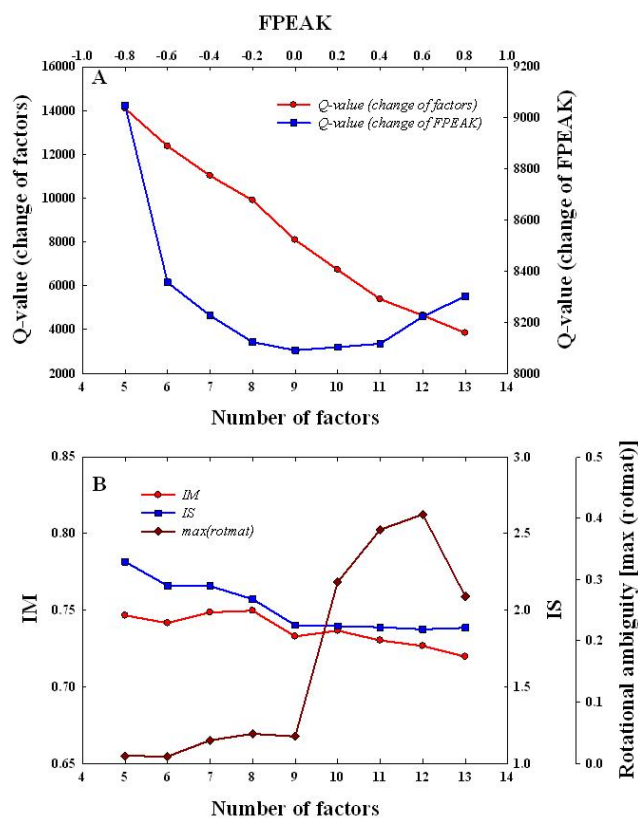


Fig. 2. (A) Q -value for the different factor solutions and the change of “FPEAK” parameter relative to the expected Q -value. The absolute Q -value (i.e., the degree of freedom of the analysis) is shown for the nine factor solutions and “FPEAK=0.0”. (B) IM (the maximum mean values of each species obtained from the scaled residuals), IS (the maximum standard deviation values of each species obtained from the scaled residuals), and rotational freedom as a function of the factors chosen in PMF.

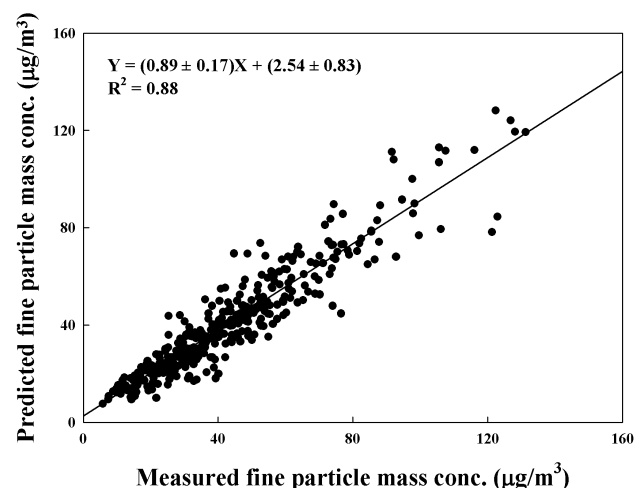


Fig. 3. Correlation between predicted and observed mass concentrations using multiple linear regression analysis.

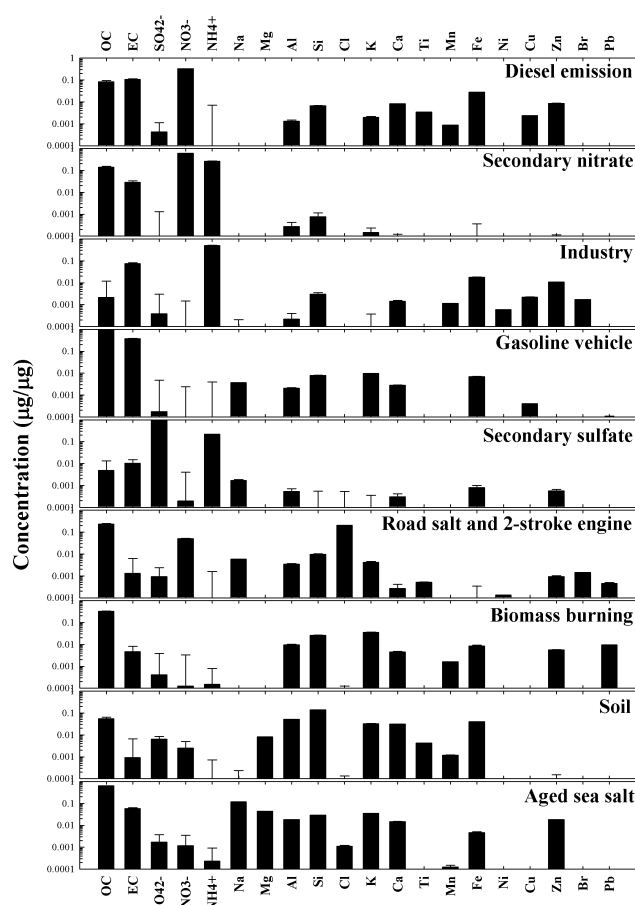


Fig. 4. Source profiles deduced from PM_{2.5} samples (prediction and error bars) in Seoul, Korea.

significant role in the particle nitrate formation in air. There are huge amounts of NH₃ in East Asia atmosphere in the spring because of fertilization of fields (Kim et al., 2006). For this reason, the average contribution of secondary nitrate factor was higher in spring compared to winter in Seoul.

The secondary sulfate factor is characterized by its high concentrations of SO₄²⁻ and NH₄⁺, and accounted for 20.5% of the PM_{2.5} mass concentration. Its mass concentration was highest during the summer, suggesting that the formation of secondary sulfate was enhanced by the increased photochemical reactivity during the summer (Song et al., 2001; Kim et al., 2007). The molar ratio of NH₄⁺ to SO₄²⁻ was 2.5 for secondary sulfate factor resolved from PMF, suggesting that (NH₄)₂SO₄ was dominated sulfate form in PM_{2.5} of Seoul. In addition, the resolved secondary sulfate factor contribution was strongly correlated with the daily concentration of HNO₃ compared to the other factors (Table 2). In general, photochemical products such as HNO₃ and secondary sulfate are strongly influenced by SO₂ and NO_x emissions from large point sources. Also, secondary sulfate tends to be higher during warmer than cooler months, reflecting in

Table 2. Pearson correlation coefficients between source contributions and meteorological data and gas concentrations.

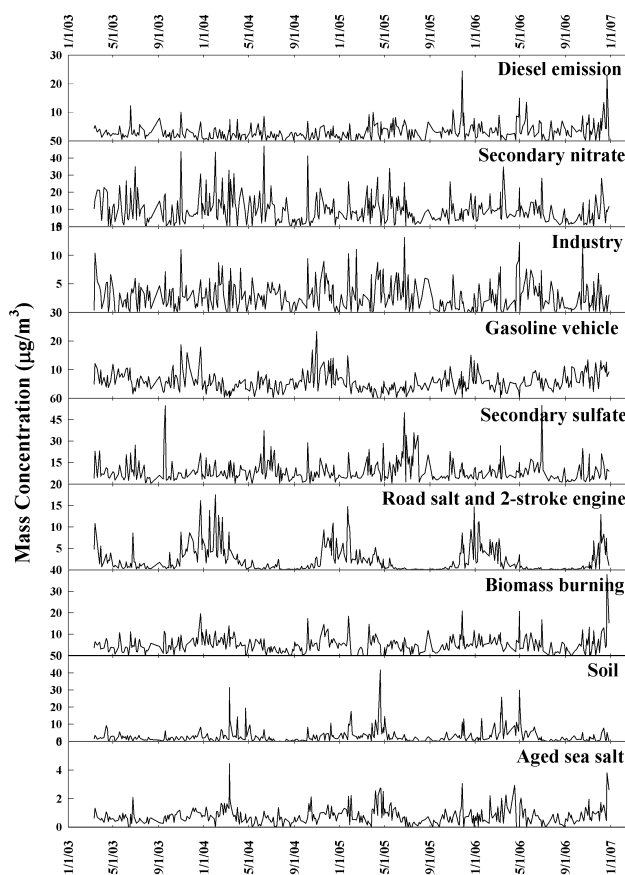
| Factor | Temp | RH | WS | SO ₂ | NO ₂ | HNO ₃ | CO |
|---------------------------|-------|-------|-------|-----------------|-----------------|------------------|------|
| Diesel emission | 0.04 | 0.00 | -0.21 | 0.35 | 0.63 | 0.28 | 0.51 |
| Secondary nitrate | -0.05 | 0.05 | -0.11 | 0.38 | 0.45 | 0.15 | 0.36 |
| Industry | 0.10 | 0.09 | -0.08 | 0.29 | 0.36 | 0.15 | 0.23 |
| Gasoline vehicle | -0.06 | -0.06 | -0.46 | 0.09 | 0.54 | -0.10 | 0.60 |
| Secondary sulfate | 0.22 | 0.23 | -0.07 | 0.30 | 0.23 | 0.50 | 0.21 |
| Road salt/2-stroke engine | -0.57 | -0.17 | -0.05 | 0.35 | 0.36 | -0.03 | 0.40 |
| Biomass burning | -0.25 | -0.06 | -0.06 | 0.45 | 0.36 | 0.15 | 0.46 |
| Soil | -0.17 | -0.23 | 0.32 | 0.16 | 0.05 | 0.06 | 0.04 |
| Aged sea salt | -0.29 | -0.19 | 0.37 | 0.25 | -0.01 | 0.02 | 0.07 |

Note that NO₂ and CO were collected in the national ambient air monitoring site in Seoul, distance 900 m from our sampling site, but SO₂ and HNO₃ were directly measured in our sampling site using annular denuder systems. Summary statistics of gas concentrations are presented in Table S2.

part the thermal stability of aerosol NH₄NO₃ in the cooler months (Liu et al., 2006). The high (NH₄)₂SO₄ production in summer leaves small amount of NH₃ for the conversion of HNO₃ to NH₄NO₃ resulting in the high correlation between the secondary sulfate factor and HNO₃.

Two types of motor vehicle factors (gasoline- and diesel-powered vehicles) were separated at the sampling site. The source contributions to the PM_{2.5} mass concentration were 17.2% for gasoline vehicles and 8.1% for diesel vehicles. The gasoline vehicle factor is characterized by a higher OC:EC concentration, while the diesel vehicle factor is characterized by a much higher EC concentration and also contribute Ca, Cu, and Zn (Lee and Hopke, 2006). Zn and Ca arise from the combustion of lubricating oil additives. Cu is emitted from the metal brake wear, and Zn has also been linked to brake linings (Lough et al., 2005; Lee and Hopke, 2006; Chellam et al., 2005). The EC/OC ratio in diesel and gasoline engine emissions is usually much higher for diesel engines than for gasoline engines in previous source apportionment studies (Table 3) and motor vehicle emission profiles studies (Table 4). In this study, the PMF resolved EC/OC ratios for diesel and gasoline vehicles were 1.4 and 0.4, respectively and this result agreed well with the studies listed in Tables 3 and 4. In general, gasoline-fueled vehicles have higher CO emission, while diesel vehicles tend to have higher NO₂ emissions. According to Pearson correlation analysis between the daily source contributions of motor vehicles deduced from PMF and the gaseous concentration data (CO and NO₂) (Table 2), there was a high correlation between gasoline vehicle factor and CO concentration, while diesel factor was highly correlated with NO₂ concentration compared to CO concentration.

At our sampling site, roads carrying a significant amount of traffic are closely situated to the east and southeast. Traffic congestion frequently occurs in these areas. Shah et al. (2004) reported that diesel vehicles operating at very slow speeds and in stop-and-go traffic produce OC:EC ratios

**Fig. 5.** Time series plots for source contributions of PM_{2.5} in Seoul, Korea.

similar to typical gasoline vehicle emissions. As much as five times more OC is generated than EC in the cold start or idle mode (stop-and-go) in heavy-duty diesel vehicles. Thus, higher OC relative to EC results could represent either gasoline or slow-moving diesel vehicles as the source. Therefore,

Table 3. Estimated EC-to-OC ratio in some important source profiles resolved by the previous receptor model studies.

| Resolved source | PMF ^a | CMB-MM ^b | CMB ^c | This study |
|------------------|------------------|---------------------|------------------|------------|
| Diesel emission | 1 | 1.33 | 1.24 | 1.4 |
| Gasoline vehicle | 0.5 | 0.025 | 0.45 | 0.4 |
| Biomass burning | 0.5 | 0.12 | 0.06–0.25 | 0.02 |
| Soil | 0.07 | 0.06 | – | 0.02 |

^a Liu et al. (2006) (study location: Southeastern US)

^b Zheng et al. (2002) (study location: Southeastern US)

^c Zheng et al. (2006) (study location: Hong Kong)

Table 4. OC and EC fractions of diesel and gasoline engine particulate matter exhaust.

| Engine type | OC | EC | EC/OC |
|---|-------|-------|----------|
| Heavy-duty diesel ^a | 19±8 | 75±10 | 2.4–7.7 |
| Heavy-duty diesel (SPECIATE) ^b | 21–36 | 52–54 | 1.4–2.7 |
| Light-duty diesel ^c | 30±9 | 61±16 | 1.1–3.7 |
| Light-duty diesel (SPECIATE) ^b | 22–43 | 51–64 | 1.2–2.9 |
| Gasoline (hot stabilized) ^a | 56±11 | 25±15 | 0.2–0.9 |
| Gasoline (“smoker” and “high emitter”) ^{a,c} | 76±10 | 7±6 | 0.01–0.2 |
| Gasoline (cold start) ^a | 46±14 | 42±14 | 0.5–1.7 |

^a Fujita et al. (1998) and Watson et al. (1998)

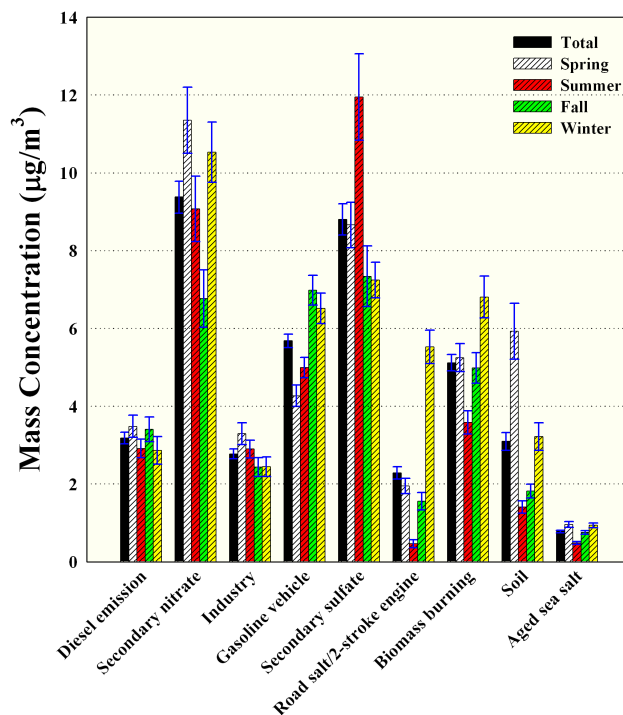
^b SPECIATE database, US Environmental Protection Agency (1999)

^c Norbeck et al. (1998)

Source: US Environmental Protection Agency (2002).

some diesel emissions could be included in the contributions of gasoline vehicles in this study. The average source contributions from gasoline and diesel emissions are compared between weekdays and the weekend in Fig. S5. The high weekday-to-weekend ratio for the two motor vehicle factors indicated that these factors were mainly from vehicles primarily operating on weekdays. Gasoline vehicle factor contributed more to the PM_{2.5} mass concentration in the winter, as shown in Fig. 6. Kim et al. (2004b) suggested that high concentrations from gasoline factors were mainly due to the increased condensation of semi-volatile compounds and from reduced mixing and dilution in the mixing layer during the winter.

The soil factor was represented by Mg, Al, Si, Ca, Ti, Fe, and K and made up 7.4% of the PM_{2.5} mass concentration. Airborne soil particles could have been resuspended in the air from sources such as road traffic, parking areas, construction sites, and wind-blown soil dust (Lee and Hopke, 2006). This factor showed seasonal variation with higher concentrations in the spring (Fig. 6). The time series contribution of this soil factor was represented in the unique high peaks that occurred during the spring at the sample site (Fig. 5). This high concentration was attributed to dust particles transported in yellow-sand events that occurred in Eastern Mongolia and

**Fig. 6.** Seasonal comparisons of source contributions to the PM_{2.5} mass concentration (mean ±95% confidence interval).

the Gobi Desert (KMA-ADC, 2007). A significant reduction in the Ca:Si value (0.52 on non yellow-sand events compared to 0.20 on yellow-sand events) for PM_{2.5} is a good yellow-sand event indicator in Beijing (He et al., 2001; Yu et al., 2006). In our study, the observed Ca:Si ratio during yellow-sand events in Seoul was 0.18–0.29, compared to 0.21–0.52 on non yellow-sand events similar to the ratios observed in Beijing. An effort was made to separate yellow-sand events from soil factor in this study, but it was not possible to separate them in an acceptable manner. As shown in Fig. S5, the high weekday-to-weekend ratio for the soil factor indicated that this factor was mainly from road traffic operating primarily during weekdays. The summer (June to August) is characterized by high humidity and heavy rain in Korea. Thus, the soil factor reflects this seasonal variation with lowest concentrations during the summer.

The biomass burning factor was characterized by high concentrations of OC, EC, and K and accounted for 12.1% of the PM_{2.5} mass concentration, with higher concentrations in the winter. This factor typically has high levels of Zn and Pb, which may be caused by residential wood burning and commercial open burning performed in winter. This factor corresponds with the field burning source profile deduced from the CMB model in a previous study of PM_{2.5} in Seoul (Park et al., 2005). In addition, several studies (Kang, et al, 2004; Park and Kim, 2004) suggested that high levels of OC and K contributing to PM_{2.5} mass concentrations observed

in Seoul may be related to biomass burning processes such as field burning after harvesting, biofuel burning for heating and cooking, and forest fires that occurred outside of the Seoul. For this reason, the biomass burning factor identified from the PMF analysis may also include local activities and regional transport from field burning.

The industry factor was characterized by high concentrations of EC, Mn, Fe, Ni, Cu, Zn, and Br. This factor made up 6.7% of the PM_{2.5} mass concentration. Non-ferrous and steel-processing factors have source profiles including the trace metals Cu, Fe, Mn, and Zn, and carbon species (Lee et al., 2006). Oil combustion for utilities and other industries is characterized by Ni and carbon fractions (Kim et al., 2004a). As shown in Fig. 1, there are national industrial complexes in the northwest (Paju) and the southwest (Sihwa and Banwol) within 30 km from the sampling site, where metal processing, non-ferrous metal smelting, and petroleum chemical process operators are located. Moreover, based on the 2005 Toxics Release Inventory (TRI) data from the Korean Ministry of the Environment, Cu, Ni, and Zn are largely emitted by primary metals and chemical processing in these industrial regions. Therefore, local industrial activities are likely contributing to the industry factor of PM_{2.5} in Seoul.

Road salt and two-stroke engine factor was identified with high concentrations of OC, NO₃⁻, Cl, and Na and accounted for 5.1% of the PM_{2.5} mass concentration. This factor is most apparent in the winter season (Fig. 5) indicating that the likely source is road salt released as a deicer on roads and other impervious surfaces close to the receptor site. Additionally, Zn, Br, and Pb were also moderately observed in this factor. Zn and Br are normally used as an additive in lubricating oil (Polissar et al., 1998). In two-stroke engines, because fuel and lubricant are mixed and burnt together in the piston chambers, Zn and Br are emitted in higher quantities from two-stroke engines (Begum et al., 2005). Also, the Seoul vehicle fleet inventory in 2006 showed that there were about 389 801 two-stroke engine vehicles (13% of total vehicles) (KNSO, 2007). Therefore, based on its profiles and seasonal patterns, this factor likely represents the mixed contribution of road salt and two-stroke engine emissions.

Lastly, aged sea salt factor was characterized by its high mass fraction of Na, Mg, K, and OC. The lack of chlorine in the profile was possibly due to the chloride displacement by acidic gases (Kim and Hopke, 2004a). This factor accounted for 2.2% of the PM_{2.5} mass concentration.

As shown in Fig. 7, daily factor contributions were analyzed using wind speeds to improve the PMF resolved factors. Figure 7 showed that most primary factor contributions increased as wind speed decreased (or as the atmospheric condition became stagnant), especially for the motor vehicles (gasoline and diesel factors). However, the contributions of soil and aged sea salt factors increased as wind speed increased possibly due to the resuspension and mixing in the air from sources during the strong wind conditions.

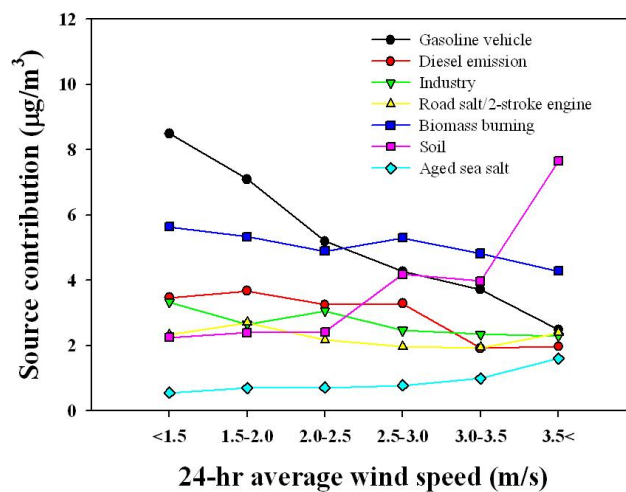


Fig. 7. Primary factor contributions as a function of wind speeds.

3.4 Conditional probability functions (CPF)

The daily estimated concentrations of the PMF-resolved factors were coupled with hourly wind direction data to locate the identified factors to local sources. The CPF plots represent the probability that specific local sources are located in certain wind direction, helping identify the impact of local point emissions to the identified sources. The directional origin of regionally transported sources may not be consistent with the local surface wind data used for the CPF plots. Figure 8 presents the CPF plots for the study results.

The CPF plot for gasoline vehicles pointed southwesterly, southerly, and southeasterly, where major highways are located (Fig. 1). Local roads run through the sampling site from the northeast to the southeast. This plot indicated that the emissions from motor vehicles operating on these highways and local roads contributed to this factor. The CPF plot for diesel emissions showed that all directions contributed to this factor, with the northwest and east being most influential. During the sampling periods, there was construction to the northwest of the site in 2006. Consequently, diesel emissions were influenced more by the northwest than other directions.

In case of soil factor, the samples influenced by transported Asian dust were omitted to avoid the influence of long range transport on CPF analysis. As shown in Fig. 8, the wind direction for the soil factor, i.e., easterly to southeasterly, likely reflected the contribution of resuspended soil particles from the local roads. The CPF plot for biomass burning factor pointed northeasterly and southeasterly where commercial and residential areas are located. This factor was likely to be influenced by local residential wood burning and commercial open burning.

The road salt and two-stroke engine factor showed high contributions coming from the southeast and moderate influences from the northwest and southwest where local roads

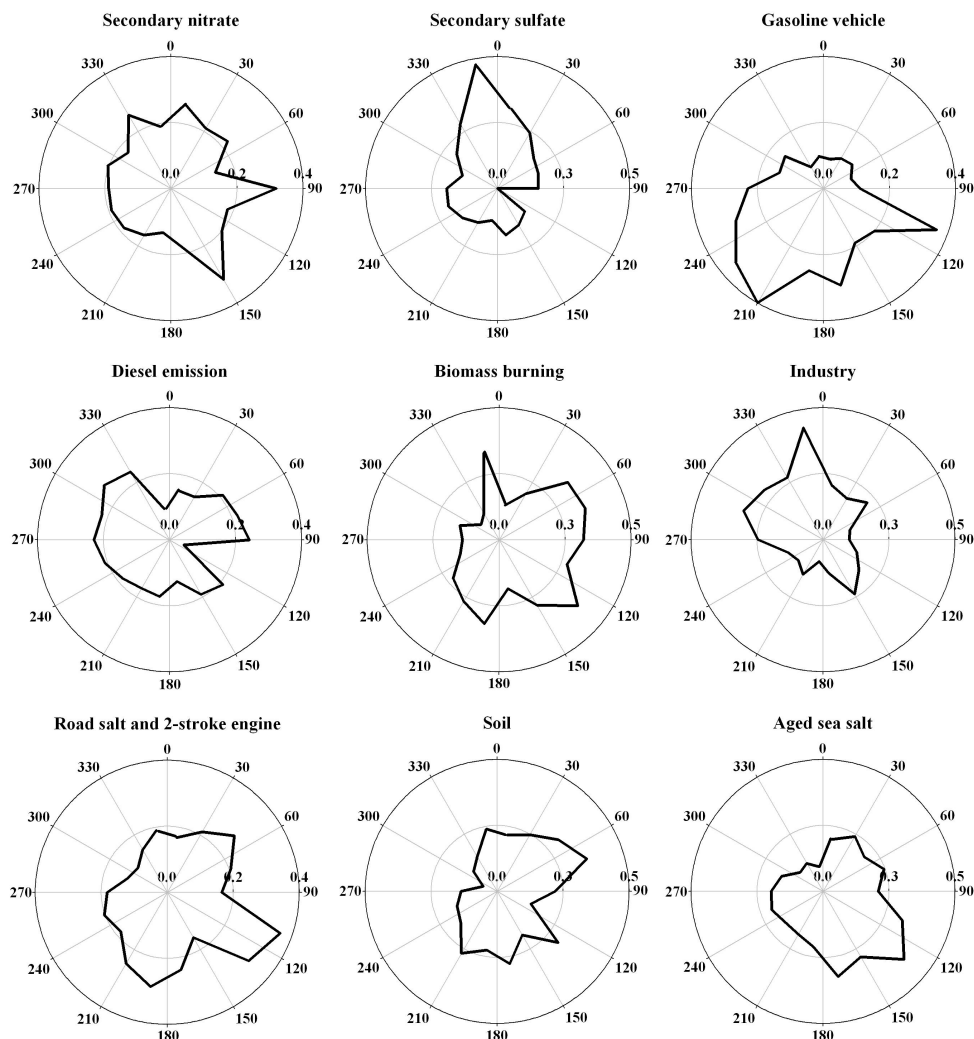


Fig. 8. CPF plots for the average source contributions deduced from PMF analysis.

are located. This result indicated that resuspended road salts used for de-icing and emissions from motorcycles operating on local roads contributed to this factor.

The aged sea salt factor pointed southeasterly. Seoul lies in a basin surrounded by mountains to the north, east, and south, and is open to the west (Kim et al., 2006). The sampling site is located to the north of the Han River (Fig. 1) and has steeper topography throughout the west and the north and gentler topography in the southeast. Fresh sea salt was likely transported from the sea to the central part of Seoul along the Han River and may have been converted from NaCl to Na-salts through the interaction with acidic gas. Therefore, it is possible that the aged sea salt was transported with the southeasterly air flow along the river to the sampling site.

The CPF plot for industrial factor shown in Fig. 8 suggested that this factor tended to impact the sampling site when transport was from the northwest, consistent with the location of major industrial complexes just northwest of Seoul.

3.5 Potential source contribution function (PSCF)

In this study, to calculate the backward trajectories, half of the mixing heights were used as the trajectory starting heights over the study period. The mixing heights were estimated by the measurement data of 2-wavelengths polarization lidar compared with potential temperature profiles from the radiosonde. Kim et al. (2007) reported that the mixing heights were approximately less than 300 m under stable conditions and about 2–3 km mixing heights were observed for well-mixed atmospheric conditions in Seoul, Korea. The spatial variation of the mixing heights calculated using HYSPLIT model 4.8 versions were about 200 m~2 km at the sampling site. Therefore, the PSCF results were calculated using all end points of trajectories generated at four different starting heights (100, 500, 1000, and 1500 m). Figure 9 showed the residence time of the backward trajectories passing through the grid cell in the PSCF grid domain, and the trajectory analysis results for four different starting

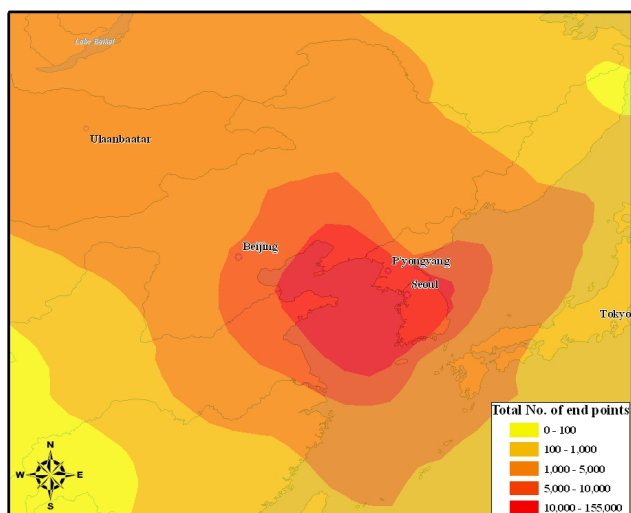


Fig. 9. Total number of end points of 5-day backward wind trajectories started at four different altitudes (100, 500, 1000, and 1500 m) during the sampling period.

heights are shown in Fig. S6. Wind in Seoul region traveled predominantly from the southwest to the northwest and then passed through China.

The PSCF plot of secondary sulfate in Fig. 10 shows the eastern coastal industrial regions in China and the Yellow Sea as potential source areas and pathways that contributed to the Seoul monitoring site. Shanghai and Hangzhou located on the east coast of China are the most developed cities with the largest gross domestic product (GDP) and energy consumption (Wang et al., 2007). The high PSCF values generated in this area may be related to the transformation and transport of SO₂ from thermal power plant, industrial, and residential emissions located in the coastal area of China. Streets et al. (2003) reported that SO₂ emissions from international shipping were 1.08 Tg in Asia and that this value was higher than the total anthropogenic emissions of SO₂ in South Korea. In addition, Kang et al. (2006) identified areas near the Yellow Sea as possible source areas for sulfate in Seoul. Thus, the high probability of secondary sulfate factor located near the Yellow Sea may originate from the emissions of international and domestic shipping and fishing vessels on the sea. The PSCF results represent both potential source directions and locations because PSCF modeling evenly distributes the weight along the path of trajectories (Hsu et al., 2003). This even weighting generates a trailing effect so that areas upwind and downwind of actual sources are also likely to be identified as possible source areas. In this study, as a result of the trailing effect, the high PSCF values of secondary sulfate on the sea were also likely to be identified as sources.

High PSCF values for secondary nitrate in Fig. 11 were found in Shanghai, Henan, Anhui, and Daqing in China. In these areas, due to rapidly growing agricultural, livestock-

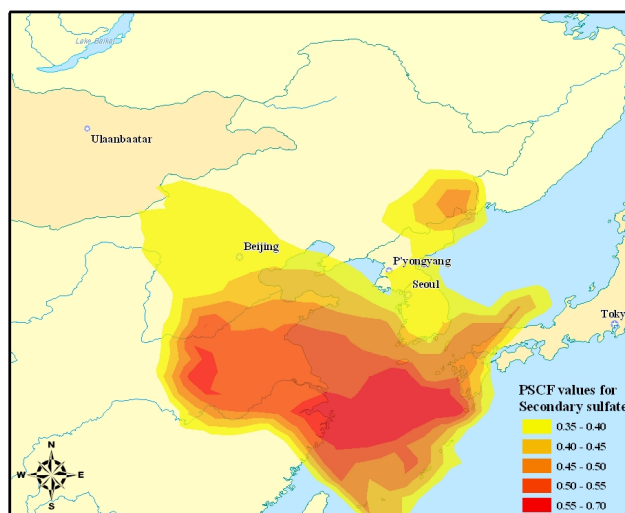


Fig. 10. Likely source area of secondary sulfate sources in Seoul, Korea over the study period using PSCF modeling.

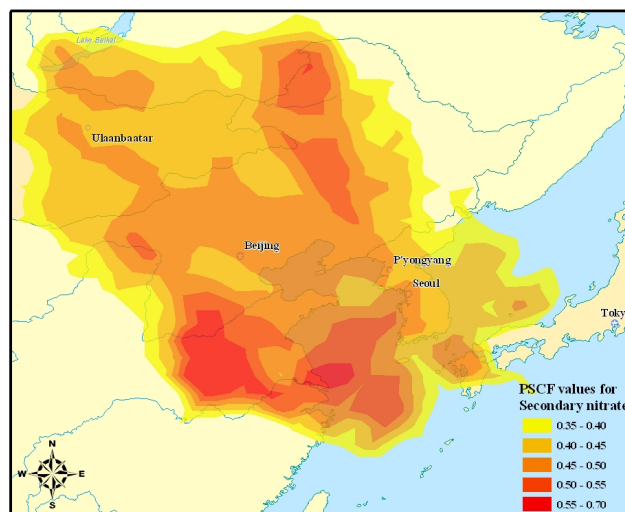


Fig. 11. Likely source area of secondary nitrate sources in Seoul, Korea over the study period using PSCF modeling.

farming, and industrial activities, the concentrations of NO_x and NH₃ have rapidly increased (Kim et al., 2006). A comparison of this result to the 2000 ammonia emissions inventory map of Asia (Streets et al., 2003) revealed that most of the “hot spots” identified by the PSCF map matched with regions of high ammonia emissions. Studies in the United States reported that area source ammonia (agricultural) emissions help transportation sources contribute significantly to regional NH₄NO₃ concentrations at downwind sites (Lee and Hopke, 2006; Kim et al., 2007; Zhao et al., 2007; Sunder Raman and Hopke, 2007). Moreover, high NH₄NO₃ formation areas in East Asia (Kim et al., 2006) are located in five eastern provinces of China (e.g., Shangdong, Anhui, Jangsu,

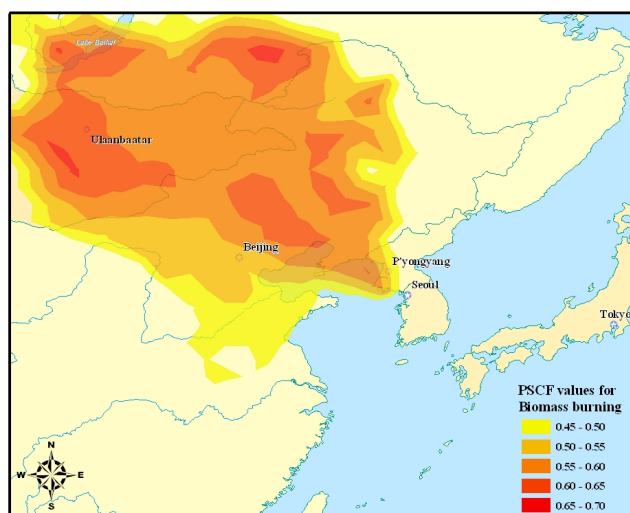


Fig. 12. Likely source area of biomass burning sources in Seoul, Korea over the study period using PSCF modeling.

Henan, and Hebei). This result suggests that the high ammonium nitrate concentrations measured in the Seoul area were likely affected by the transport of ammonium nitrate that was formed over the high ammonia source regions, or elsewhere, during transport.

The sulfate and nitrate maps show the contrast in seasonality of secondary particle formation and that PSCF reflects the combination of emissions, formation, and transport. In summer when photochemical activity is high and SO₂ conversion is more rapid, the prevailing winds are from the southwest. In the winter, when the cooler temperatures lead to the formation of particulate nitrate, the winds are from the northwest. During this period, conversion rates for SO₂ are low and thus, northerly winds do not contribute to the highest concentrations of particulate sulfate. Thus, known SO₂ source areas in Northern China do not significantly contribute to sulfate in Seoul. In the same way, NO_x source areas of Southern China do not contribute to particulate nitrate.

Biomass burning was predominant in the northwest, and its high PSCF values were located along the Russian borders with Mongolia and China (Fig. 12). Siberia and other parts of Eastern Russia are the major boreal forest fire areas where a huge amount of carbon emissions and smoke plumes occur each year. Extensive fire activities occurred during the early summer in 2003 across the Siberian border in Russia between the Amur and Lena Rivers and east of Lake Baikal. Smoke plumes from these Russian forest fires were often transported to Northeast Asia, through Mongolia, Eastern China, and Korea (Lee et al., 2005). In this study, the regions with high PSCF values for biomass burning were consistent with burned biomass areas identified using satellite data and a biomass burning emission inventory (Jaffe et al., 2004). Therefore, biomass burning may be influenced by local activities and long-range transport in Seoul.

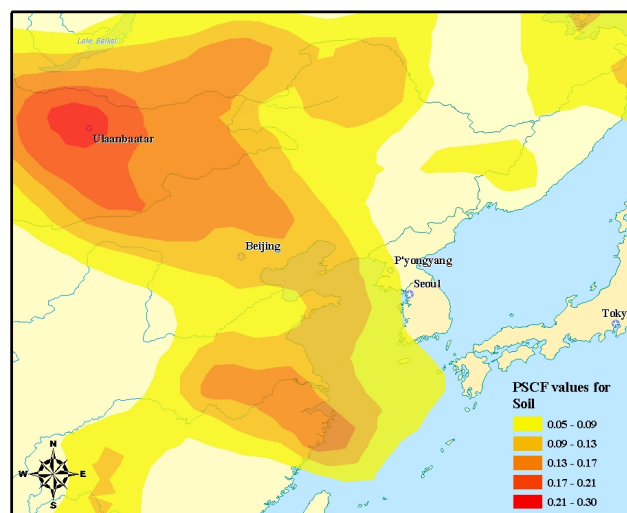


Fig. 13. Likely source area of soil sources in Seoul, Korea over the study period using PSCF modeling.

The criterion value of PSCF for soil was set to the upper 10th percentile of the source concentration because the contribution of soil was much higher during the 29 yellow-sand events that were observed during this sampling period. As shown in Fig. 13, the high PSCF values for soil at the sampling site were attributed to the Gobi Desert and the Mongolian plateau. The Gobi Desert is the second largest desert in China and is assumed to be the main source of yellow-sand transported to Korea. As previously described, the extremely high soil impacts of PM_{2.5} in Seoul were mainly due to yellow-sand events.

4 Conclusions

PM_{2.5} and its chemical constituents collected at a centrally located urban monitoring site in Seoul, Korea were measured every third day from March 2003 to December 2006, and source identification was undertaken using PMF. A total of 393 observations were made during the sampling period, and 20 particulate chemical species were analyzed. In this study, nine factors were identified providing realistic sources and interesting insights into their contributions to the ambient aerosol. The PMF predicted that the major contributors of PM_{2.5} were secondary nitrate (20.9%), secondary sulfate (20.5%), gasoline-fueled vehicles (17.2%), and biomass burning (12.1%) followed by lesser contributions from diesel emissions (8.1%), soil (7.4%), industry (6.7%), road salt and two-stroke engine (5.1%), and aged sea salt (2.2%). By coupling wind direction data with the daily source contributions deduced from the PMF, the relative influence of distant and local PM_{2.5} sources in Seoul were explored. Effects of regional sources were also found using PSCF analysis for the PMF-resolved source contributions. The influences of local

point sources such as motor vehicles, road salt, residential open burning, and non-ferrous smelting were clearly identified at the monitoring sites. Both secondary sulfate and secondary nitrate factors were regional sources. The eastern coastal industrial area of China was a potential source region for secondary sulfate. The high contribution of secondary nitrate observed in Seoul was likely influenced by ammonium emissions from large agricultural regions in China, including the provinces of Shanghai, Henan, Anhui, and Daqing. Regional transport of biomass burning occurred within the Russian borders, including Siberia and other parts of Eastern Russia, and the northeast plain of China was also identified in this study. The long-range transport from yellow-sand events originating in the Gobi Desert and the Mongolian plateau influenced the high soil impacts of PM_{2.5} in Seoul area. This study suggested that the long-range transport must be considered to control the level of PM_{2.5} mass concentration in Seoul, Korea.

Acknowledgements. This work was supported by the Ministry of Environment, Republic of Korea (Ecotechnopia 091-071-057, 09001-0020-0). The authors gratefully acknowledge the NOAA Air Resources Laboratory (ARL) for the provision of the HYSPLIT transport and dispersion model and/or READY website (<http://www.arl.noaa.gov/ready.html>) used in this publication.

Edited by: U. Lohmann

References

- Ashbaugh, L. L., Malm, W. C., and Sadeh, W. Z.: A residence time probability analysis of sulfur concentrations at Grand Canyon National Park, *Atmos. Environ.*, 19(18), 1263–1270, 1985.
- Begum, B. A., Biswas, S. K., Kim, E., Hopke, P. K., and Khaliqzaman, M.: Investigation of sources of atmospheric aerosol at a hot spot area in Dhaka, Bangladesh, *JAPCA J. Air Waste Ma.*, 55(2), 227–240, 2005.
- Birch, M. E. and Cary, R. A.: Elemental carbon-based method for monitoring occupational exposures to particulate diesel exhaust, *Aerosol Sci. Tech.*, 25(3), 221–241, 1996.
- Chang, S. N., Hopke, P. K., Gordon, G. E., and Rheingrover, S. W.: Target-transformation factor analysis of airborne particle samples selected by wind-trajectory analysis, *Aerosol Sci. Tech.*, 8(1), 63–80, 1988.
- Chellam, S., Kulkarni, P., and Fraser, M. P.: Emission of Organic Compounds and Trace Metals in Fine Particulate matter from Motor Vehicles: a Tunnel Study in Houston, Texas, *JAPCA J. Air Waste Ma.*, 55(1), 60–72, 2005.
- Dockery, D. W., Pope, C. A., Xiping, X., Spengler, J. D., Ware, J. H., Fay, M. E., Ferris Jr., B. G., and Speizer, F. E.: An association between air pollution and mortality in six US cities, *New Engl. J. Med.*, 329(24), 1753–1759, 1993.
- Draxler, R. R. and Rolph, G. D.: HYSPLIT4 (Hybrid Single-Particle Lagrangian Integrated Trajectory) Model, NOAA Air Resources Laboratory, Silver Spring, MD, available at: <http://www.arl.noaa.gov/ready/hysplit4.html>, 2007.
- Fujita, E., Watson, J. G., Chow, J. C., Robinson, N. F., Richards, L. W., and Kumar, N.: Northern front range air quality study, volume C: source apportionment and simulation methods and evaluation, Reno, NV: Desert Research Institute, prepared for Colorado State University, Cooperative Institute for Research in the Atmosphere, 1998.
- Han, Y. J., Holsen, T. M., Hoke, P. K., Cheong, J. P., Kim, H., and Yi, S. M.: Identification of source locations for atmospheric dry deposition of heavy metals during yellow-sand events in Seoul, Korea in 1998 using hybrid receptor models, *Atmos. Environ.*, 38(31), 5353–5361, 2004.
- Han, Y. -J., Holsen, T. M., and Hopke, P. K.: Estimation of source locations of total gaseous mercury measured in New York State using trajectory-based models, *Atmos. Environ.*, 41(28), 6033–6047, 2007.
- He, K., Yang, F., Ma, Y., Zhang, Q., Yao, X., Chan, C. K., Cadle, S., Chan, T., and Mulawa, P.: The characteristic of PM_{2.5} in Beijing, China, *Atmos. Environ.*, 35(29), 4959–4970, 2001.
- Hopke, P. K.: Receptor modeling for air quality management, Elsevier Press, Amsterdam, The Netherlands, 7, 1991.
- Hopke, P. K., Barrie, L. A., Li, S.-M., Cheng, M.-D., Li, C., and Xie, Y.: Possible sources and preferred pathways for biogenic and non-sea salt sulfur for the high Arctic, *J. Geophys. Res.*, 100(D8), 16595–16603, 1995.
- Hsu, Y.-K., Holsen, T. M., and Hopke, P. K.: Comparison of hybrid receptor models to locate PCB sources in Chicago, *Atmos. Environ.*, 37(4), 545–562, 2003.
- Hwang, I. J. and Hopke, P. K.: Estimation of source apportionment and potential source locations of PM_{2.5} at a west coastal IMPROVE site, *Atmos. Environ.*, 41(3), 506–518, 2007.
- Jaffe, D., Bertshci, I., Jaegle, L., Novelli, P., Reid, J. S., Tanimoto, H., Vingarzan, R., and Westphal, D. L.: Long-range transport of Siberian biomass burning emissions and impact on surface ozone in western North America, *Geophys. Res. Lett.*, 31, L16106, doi:10.1029/2004GL020093, 2004.
- Kang, C. M., Lee, H. S., Kang, B. W., Lee, S. K., and Sunwoo, Y.: Chemical characteristics of acidic gas pollutants and PM_{2.5} species during hazy episodes in Seoul, South Korea, *Atmos. Environ.*, 38(28), 4749–4760, 2004.
- Kang, C. M., Kang, B. W., and Lee, H. S.: Source identification and trends in concentrations of gaseous and fine particulate principal species in Seoul, South Korea, *J. Air Waste Ma.*, 56(7), 911–921, 2006.
- Kim, E., Hopke, P. K., and Edgerton, E. S.: Source identification of Atlanta aerosol by positive matrix factorization, *J. Air Waste Ma.*, 53(6), 731–739, 2003.
- Kim, E. and Hopke, P. K.: Improving source identification of fine particles in a rural northeastern US area utilizing temperature-resolved carbon fractions, *J. Geophys. Res.*, 109, D09204, doi:10.1029/2003JD004199, 2004a.
- Kim, E. and Hopke, P. K.: Source apportionment of fine particles at Washington, DC utilizing temperature resolved carbon fractions, *J. Air Waste Ma.*, 54(7), 773–785, 2004b.
- Kim, E., Hopke, P. K., and Edgerton, E. S.: Improving source identification of Atlanta aerosol using temperature resolved carbon fractions in Positive Matrix Factorization, *Atmos. Environ.*, 38(20), 3349–3362, 2004a.
- Kim, E., Hopke, P. K., Lason, T. V., Mayjut, N. N., and Lewtas, J.: Factor analysis of Seattle fine particles, *Aerosol Sci. Tech.*, 38(7), 724–738, 2004b.
- Kim, H. S., Huh, J. B., Hopke, P. K., Holsen, T. M., and Yi, S. M.:

- Characteristics of the major chemical constituents of PM_{2.5} and smog events in Seoul, Korea in 2003 and 2004, *Atmos. Environ.*, 41(32), 6762–6770, 2007.
- Kim, J. Y., Song, C. H., Ghim, Y. S., Won, J. G., Yoon, S. C., Carmichael, G. R., and Woo, J.-H.: An investigation on NH₃ emissions and particulate NH₄⁺-NO₃⁻ formation in East Asia, *Atmos. Environ.*, 40(12), 2139–2150, 2006.
- Kim, M. W., Deshpande, S. R., and Crist, K. C.: Source apportionment of fine particulate matter (PM_{2.5}) at a rural Ohio River Valley site, *Atmos. Environ.*, 41(39), 9231–9243, 2007.
- Kim, S. W., Yoon, S. C., Won, J. G., and Choi, S. C.: Ground-based remote sensing measurements of aerosol and ozone in an urban area: A case study of mixing height evolution and its effect on ground-level ozone concentrations, *Atmos. Environ.*, 41(33), 7069–7081, 2007.
- KMA-ADC, Korea Meteorological Administration, Asian Dust Center, available at: <http://www.kma.go.kr/>, 2007.
- KNSO, Korea National Statistical Office: Korean Statistical Information Service, available at: <http://www.kosis.kr/>, 2007.
- Lanz, V. A., Alfarra, M. R., Baltensperger, U., Buchmann, B., Hueglin, C., and Prévôt, A. S. H.: Source apportionment of sub-micron organic aerosols at an urban site by factor analytical modelling of aerosol mass spectra, *Atmos. Chem. Phys.*, 7, 1503–1522, 2007, <http://www.atmos-chem-phys.net/7/1503/2007/>.
- Lee, J. H., Hopke, P. K., and Turner, J. R.: Source Identification of Airborne PM_{2.5} at the St. Louis-Midwest Supersite, *J. Geophys. Res.*, 111, D10S10, doi:10.1029/2005JD006329, 2006.
- Lee, E., Chan, C. K., and Paatero, P.: Application of positive matrix factorization in source apportionment of particulate pollutants in Hong Kong, *Atmos. Environ.*, 33(19), 3201–3212, 1999.
- Lee, H. S., Kang, C. M., Kang, B. W., and Lee, S. W.: A study on the PM_{2.5} source characteristics affecting the Seoul area using a chemical mass balance receptor model, *J. KOSAE*, 21(3), 329–341, 2005 (in Korean).
- Lee, J. H. and Hopke, P. K.: Apportioning sources of PM_{2.5} in St. Louis, MO using speciation trends network data, *Atmos. Environ.*, 40, SUP2, S360–S377, 2006.
- Lee, K. H., Kim, J. E., Kim, Y. J., and Hoyningen-Huene, W.: Impact of the smoke aerosol from Russian forest fires on the atmospheric environment over Korea during May 2003, *Atmos. Environ.*, 39(1), 85–99, 2005.
- Lee, P. K., Brook, J. R., Dabek-Zlotorzynska, E., and Mabury, S. A.: Identification of the major sources contribution to PM_{2.5} observed in Toronto, *Environ. Sci. Technol.*, 37, 21, 4831–4840, 2003.
- Liu, W., Wang, Y., Russell, A. G., and Edgerton, E. S.: Enhanced source identification of Southeast aerosols using temperature resolved carbon fractions and gas phase components, *Atmos. Environ.*, 40, SUP2, S445–466, 2006.
- Lough, G. C., Schauer, J. J., Park, J.-S., Shafer, M. M., Deminter, J. T., and Weinstein, J. P.: Emissions of Metals Associated with Motor Vehicle Roadways. *Environ. Sci. Technol.*, 39(3), 826–836, 2005.
- Malinowski, E. R.: *Factor analysis in chemistry*, John Wiley and Sons, Inc, 2002.
- MOE, Ministry of Environment, Korea: Toxics Release Inventory in Korea 2005, available at: <http://www.me.go.kr/>, 2007 (in Korean).
- MOE, Ministry of Environment, Korea: Regional waste inventory in 2006, available at: <http://www.me.go.kr/>, 2007 (in Korean).
- Norbeck, J. M., Durbin, T. D., and Truex, T. J.: Measurement of primary particulate matter emissions from light-duty motor vehicles, Riverside, CA, University of California, College of Engineering, Center for Environmental Research and Technology, prepared for Coordinating Research Council, Inc. and South Coast Air Quality Management District, 1998.
- Paatero, P.: Least squares formulation of robust, non-negative factor analysis, *Chemometr. Intell. Lab.*, 37(1), 23–35, 1997.
- Paatero, P. and Tapper, U.: Analysis of different modes of factor analysis as least squares fit problems, *Chemometr. Intell. Lab.*, 18(22), 183–194, 1993.
- Paatero, P. and Tapper, U.: Positive matrix factorization: a non-negative factor model with optimal utilization of error estimates of data values, *Environmetrics*, 5(2), 111–126, 1994.
- Paatero, P., Hopke, P. K., Song, X. H., and Ramadan, Z.: Understanding and controlling rotations in factor analytic models, *Chemometr. Intell. Lab.*, 60(1), 253–264, 2002.
- Paatero, P. and Hopke, P. K.: Discarding or downweighting high noise variables in factor analytic models, *Anal. Chim. Acta*, 490(1), 277–289, 2003.
- Park, S. S. and Kim, Y. J.: Source contributions to fine particulate matter in an urban atmosphere, *Chemosphere*, 59(22), 217–226, 2005.
- Pekney, N. J., Davidson, C. I., Zhou, L., and Hopke, P. K.: Application of PSCF and CPF to PMF-modeled sources of PM_{2.5} in Pittsburgh, *Aerosol Sci. Technol.*, 40(10), 952–961, 2006.
- Polissar, A. V., Hopke, P. K., Paatero, P., Malm, W. C., and Sisler, J. F.: Atmospheric aerosol over Alaska 2. Elemental composition and sources, *J. Geophys. Res.*, 103(D15), 19045–19057, 1998.
- Polissar, A. V., Hopke, P. K., and Harris, J. M.: Source regions for atmospheric aerosol measured at Barrow, Alaska, *Environ. Sci. Technol.*, 35(21), 4214–4226, 2001.
- Schwartz, J., Laden, F., and Zanobetti, A.: The concentration-response relation between PM_{2.5} and daily deaths, *Environ. Health Persp.*, 110(10), 1025–1029, 2002.
- Seinfeld, J. H. and Pandis, S. N.: *Atmospheric Chemistry and Physics*, Wiley/Interscience, 1998.
- Shah, S. D., Cocker III, D. R., Wayne, J. M., and Norbeck, J. M.: Emission rates of particulate matter and elemental and organic carbon from in-use diesel engines, *Environ. Sci. Technol.*, 38(9), 2544–2550, 2004.
- Song, X.-H., Polissar, A. V., and Hopke, P. K.: Source of fine particle composition in the northeastern US, *Atmos. Environ.*, 35(31), 5277–5286, 2001.
- Song, Y., Zhang, Y., Xie, S., Zeng, L., Zheng, M., Salmon, L. G., Shao, M., and Slanina, S.: Source apportionment of PM_{2.5} in Beijing by positive matrix factorization, *Atmos. Environ.*, 40(8), 1526–1537, 2006.
- Streets, D. G., Bond, T. C., Carmichael, G. R., Fernandes, S. D., Fu, Q., He, D., Klimont, Z., Nelson, S. M., Tsai, N. Y., Wang, M. Q., Woo, J.-H., and Yarber, K. F.: An inventory of gaseous and primary aerosol emissions in Asia in the year 2000, *J. Geophys. Res.*, 108(D21), 8809, doi:10.1029/2002JD003093, 2003.
- Sunder Raman, R. and Hopke, P. K.: Source apportionment of fine particles utilizing partially speciated carbonaceous aerosol data at two rural locations in New York State, *Atmos. Environ.*, 41(36), 7923–7939, 2007.
- Ulbrich, I. M., Canagaratna, M. R., Zhang, Q., Worsnop, D. R.,

- and Jimenez, J. L.: Interpretation of organic components from Positive Matrix Factorization of aerosol mass spectrometric data, *Atmos. Chem. Phys.*, 9, 2891–2918, 2009, <http://www.atmos-chem-phys.net/9/2891/2009/>.
- US Environmental Protection Agency: SPECIATE, Washington, DC: Technology Transfer Network-Clearinghouse for Inventories & Emissions Factors, available at: <http://www.epa.gov/ttn/chief/software/speciate/index.html>, 1999.
- US Environmental Protection Agency: Health assessment document for diesel engine exhaust, Washington, DC: Office of Research and Development, report no. EPA/600/8-90/057, 2002.
- US Federal Register: National ambient air quality standards for particulate matter, Federal Register 40 CFR Part 51, 72, 79, 20587, 2007.
- Viana, M., Kuhlbusch, T. A. J., Querol, X., Alastuey, A., Harrison, R. M., Hopke, P. K., Winiwarer, W., Vallius, A., Szidat, S., Prevot, A. S. H., Hueglin, C., Bloemen, H., Wahlin, P., Vecchi, R., Miranda, A. I., Kasper-Giebl, A., Maenhaut, W., and Hitzenberger, R.: Source apportionment of particulate matter in Europe: A review of methods and results, *J. Aerosol Sci.* 39(10), 827–849, 2008.
- Wang, Y., Zhong, G., Tang, A., Zhang, W., Sun, Y., Wang, Z., and An, Z.: The evolution of chemical components of aerosols at five monitoring sites of China during dust storms, *Atmos. Environ.*, 41(5), 1091–1106, 2007.
- Watson, J. G., Fujita, E. M., Chow, J. C., Zielinska, B., Richards, L. W., Neff, W., and Dietrich, D.: Northern front range air quality study final report, Reno, NV: Desert Research Institute, prepared for Colorado State University, Cooperative Institute for Research in the Atmosphere, 1998.
- Watson, J. G., Chow, J. C., and Fujita, E. M.: Review of volatile organic compound source apportionment by chemical mass balance, *Atmos. Environ.*, 35(9), 1567–1584, 2001.
- Zheng, M., Cass, G. G., Schauer, J. J., and Edgerton, E. S.: Source apportionment of PM_{2.5} in the southeastern United States using solvent-extractable organic compounds as tracers, *Environ. Sci. Technol.*, 36(11), 2361–2371, 2002.
- Zhao, W., Hopke, P. K., and Zhou, L.: Spatial distributions for origins of nitrate and sulfate in upper-Midwestern United States, *Atmos. Environ.*, 41, 1831–1847, 2007.